THE JOURNAL OF PHYSICAL CHEMISTRY A

Article

Cite This: J. Phys. Chem. A XXXX, XXX, XXX−XXX

pubs.acs.org/JPCA

Prediction of a Nonvalence Temporary Anion Shape Resonance for a Model $(H_2O)_4$ System

Published as part of The Journal of Physical Chemistry virtual special issue "Abraham Nitzan Festschrift".

Arailym Kairalapova and Kenneth D. Jordan*

Department of Chemistry, University of Pittsburgh, Pittsburgh, Pennsylvania 15260, United States

Daniel N. Maienshein, Mark C. Fair, and Michael F. Falcetta

Department of Chemistry, Grove City College, Grove City, Pennsylvania 16127, United States

ABSTRACT: Ab initio calculations are used to demonstrate the existence of a nonvalence temporary anion shape resonance for a model $(H_2O)_4$ cluster system with no net dipole moment. The cluster is composed of two water dimers, the distance between which is varied. Each dimer possesses a weakly bound nonvalence anion state. For large separations of the dimer subunits, there are two bound nonvalence anion states (of A_g and B_{2u} symmetry) corresponding to the symmetric and asymmetric combinations of the nonvalence anion states of the two dimer subunits. As the separation between the dimer subunits is decreased, the B_{2u} anion increases in energy and becomes a temporary anion shape resonance. The real part of the resonance energy is determined as a function of the distance between the dimers and is found to increase monotonically from just above threshold to 28 meV for the range of geometries considered. Over this same range of geometries, the resonance half-width varies from 0 to 21 meV. The B_{2u} anion, both when bound and when temporary, has a very diffuse charge distribution. The effective radial potential for the interaction of the excess electron with the cluster has a barrier at large distance arising from the electron−quadrupole interaction in combination with the repulsive angular momentum ($l = 1$) contribution. This barrier impacts both the resonance energy and its lifetime.

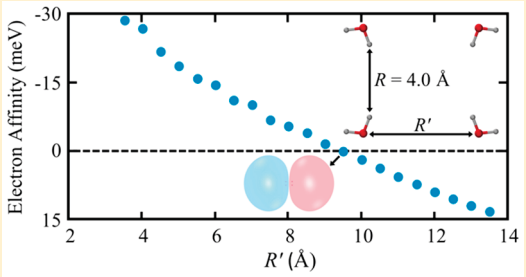

1. INTRODUCTION

Anion states formed by electron capture into normally unfilled valence orbitals are of importance in a wide range of chemical and biological processes. Less well-known in the chemistry community at large are anions that result from electron capture into diffuse nonvalence orbitals, with a combination of long-range electrostatic and correlation effects being responsible for the electron binding. The most widely studied class of nonvalence anions are dipole-bound anions in which the electrostatic attraction to the molecular dipole potential alone can bind the excess electron, although correlation effects can cause a significant increase in the electron binding energy (EBE).[1−3] (Here we adopt the sign convention of a positive EBE when the anion is bound, i.e., energetically below the electronic ground state of the neutral.) Recently, several examples of another class of nonvalence anions, which we refer to as nonvalence correlation-bound (NVCB) anions, have also been demonstrated.[4−11] For these, long-range correlation effects are essential for the binding of the excess electron. Although the excess electron in dipole-bound and NVCB anions occupies a very diffuse orbital, such anion states can be important in chemical processes, e.g., acting as doorway states for formation of valence anions.[9,10,12] Specifically, geometrical distortion can lead to mixing (via the electronic Hamiltonian) of nonvalence and valence anion states, which may be of different symmetry in the undistorted molecule.[13] Additionally, molecular anions in which the electrostatic attraction of the excess electron to the quadrupole moment plays a role in the binding of the excess electron have been investigated,[14−17] as have model systems in which the electron−quadrupole interaction makes a significant contribution to the EBE.[5,18,19] We note that there are several studies that interpret experiments in terms of "quadrupole-bound" anions.[16,20−22] However, for many of these systems (e.g., *trans*-succinonitrile[23]), the anion is not bound in the Koopmans' theorem (KT) approximation,[24] which means that the quadrupole moment alone is not large enough to bind the excess electron. Rather, it is the combination of electron correlation effects and the electrostatic potential associated with the quadrupole moment that gives rise to the electron binding. We believe that such anions are better classified as NVCB. In the case of CS_2,

Received: December 10, 2018
Revised: March 5, 2019
Published: March 6, 2019

DOI: 10.1021/acs.jpca.8b11881
J. Phys. Chem. A XXXX, XXX, XXX−XXX

which has been proposed to have a quadrupole-bound anion,[20] it appears that the state involved is actually valence-like.[25]

In addition to bound anions, atoms and molecules can possess anion states that lie energetically above the ground state of the neutral species. These anions are termed temporary as they are subject to decay by electron autodetachment, and they appear as resonances in electron scattering cross sections.[26,27] Temporary anions (TAs) are involved in a range of processes including chemical bond breaking and vibrational and electronic excitation. Generally, low-energy TAs are associated with electron capture into unfilled valence orbitals, with the trapping mechanism being due to an angular momentum barrier in the effective radial potential.[26,27] Such TAs are also referred to as shape resonances because the trapping is due to the shape of the electron−atom or electron−molecule potential. Another type of TA involves trapping of an excess electron in the potential of an electronically excited state,[26] but these will not be considered further here.

In the present study, we examine the possibility of the existence of nonvalence correlation-assisted TA shape resonances for a cluster with no dipole moment but with a sizable quadrupole moment. We use the label "correlation-assisted" to indicate that electron correlation effects play a major role in establishing the energy and lifetime of the anion. In our search for a nonvalence TA, we consider a model $(H_2O)_4$ system that, for a range of geometries, possesses a NVCB anion with a p-like, i.e., $l = 1$, leading partial wave but that can be distorted to geometries for which this anion is "pushed" into the continuum of the neutral species plus a free electron. We note that nonvalence TA resonances have been reported for molecules with sizable dipole moments.[28−30]

2. $(H_2O)_4$ MODEL SYSTEM AND COMPUTATIONAL DETAILS

The $(H_2O)_4$ cluster model, which was employed in our earlier study of NVCB anions,[5] is shown in Figure 1. By design, the

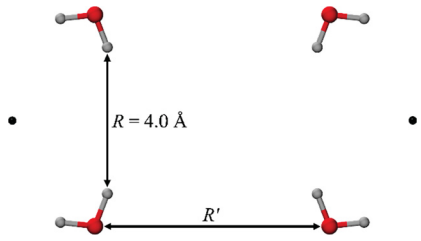

Figure 1. $(H_2O)_4$ cluster model. R is fixed to 4.0 Å, while R' is varied. The black dots indicate the locations of the supplemental sets of diffuse basis functions, which are located at $\pm(R'/2 + 2.27)$ in Å.

monomers in this model are arranged so that there is no net dipole and the leading permanent moment is a quadrupole. The absence of a dipole is essential for the existence of a low-energy resonance with a leading $l = 1$ partial wave. Although this arrangement of monomers would not be observed experimentally, our earlier work demonstrated that this is a useful model for exploring the interplay of electrostatics and electron correlation in nonvalence anion states. In the present study, we fix the distance R and vary the distance R' defined in Figure 1. Thus, we are varying the separation between two water dimers (albeit with geometrical structures far from equilibrium). The individual dimers have a dipole moment of 2.1 D (MP2[31] level with the aug-cc-pVTZ[32,33] Gaussian-type orbital basis set). As a result, in isolation and assuming the validity of the Born−Oppenheimer approximation, each dimer subunit has a dipole-bound anion. In the KT approximation, the EBE is approximated by the negative of the energy of the appropriate virtual orbital from a Hartree−Fock (HF) calculation on the neutral species (although care has to be exercised when applying the KT approximation to unbound virtual orbitals). In the KT approximation, the dimer is calculated to have a miniscule EBE of 0.9 meV. There is only a small increase of the EBE to 1.0 meV when allowing for relaxation effects by calculating the difference in the HF energies of the anion and neutral (the so-called ΔSCF approximation). Thus, at large R' values, the $(H_2O)_4$ cluster model has two, nearly degenerate, bound anion states, one of A_g and the other of B_{2u} symmetry, resulting from the symmetric and asymmetric linear combinations of the bound states of the two dimer subunits in the tetramer. At the KT level, these become unbound for R' values less than about 40 Å (A_g) and 70 Å (B_{2u}). Similar crossing points are found in the ΔSCF approximation. However, we know from our earlier study of this model system that inclusion of electron correlation effects leads to a large increase in the EBE of the A_g anion state, in fact, resulting in a stable anion even at geometries at which the HF method fails to bind the excess electron. We anticipate, therefore, that inclusion of correlation effects will prove important in determining whether the B_{2u} anion is bound or metastable at different R' values.

In order to include electron correlation effects in the calculation of the energies of the A_g and B_{2u} nonvalence anion states of the $(H_2O)_4$ model as a function of R', we use the electron attachment equation-of-motion coupled-cluster singles and doubles (EOM-CCSD) method[34] as implemented in the CFOUR program[35] together with flexible Gaussian-type orbital (GTO) basis sets and the frozen core approximation. The EOM-CCSD method has been found to provide accurate characterization of both valence and nonvalence bound anion states as well as of valence-type TA states provided that sufficiently flexible basis sets are employed.[5,36,37] In the present study, we use the aug-cc-pVTZ basis set for the atoms augmented with nonatom-centered sets of diffuse s (or s and p) Gaussian-type functions located on the positive dipole side of each dimer, as shown in Figure 1. Well-converged EBEs for the bound anions were obtained from calculations employing supplemental sets consisting of seven s or seven s plus seven p functions, with the largest exponent being 0.025 and with successive exponents reduced by a factor of $\sqrt{10}$. The location of the supplemental basis functions relative to the O atoms was determined by maximizing the EOM-CCSD value of the EBE of the A_g anion at $R' = 13.5$ Å. This optimization located the centers for the supplemental basis sets 2.27 Å farther from the origin along the R' coordinate than the oxygen atoms. In calculations at other R' values, the locations of the centers of the supplemental diffuse functions, relative to the dimers, were held fixed at this value. EOM-CCSD calculations also showed that omission of the p functions from the supplemental sets made little impact on the EBEs, and as a result, supplemental sets with only s functions were used for the majority of the calculations. For the TA, it was necessary to add two additional s functions with exponents of 0.250 and 0.079 to the supplemental sets, as will be described below. For consistency, these extra functions are retained in the calculations of the bound anion states when using supplemental sets with only s functions, although they do not make an important

DOI: 10.1021/acs.jpca.8b11881
J. Phys. Chem. A XXXX, XXX, XXX−XXX

contribution to the EBEs. We note that in designing the basis sets for characterizing the anion states of the $(H_2O)_4$ model we first considered using only a single set of supplemental diffuse functions located at the center of mass but found that to achieve well-converged results with such basis sets it was necessary to employ a basis as large as aug-cc-pV5Z[32,33] on the atoms and to include functions through f in the supplemental set. By using the two-center expansion for the supplemental functions described above, we were able to achieve well-converged EBEs with far fewer basis functions.

3. RESULTS

For the $(H_2O)_2$ dimer with the geometry of our model, the EOM-CCSD calculations carried out using the aug-cc-pVTZ basis set plus a single 7s7p set of supplemental functions gave a binding energy of 38 meV for the A_g anion, in contrast to the 0.9 meV value obtained at the KT level of theory. The KT calculations failed to bind the excess electron with the supplemental set containing only s functions, but the EBE obtained using the EOM method was changed little upon omission of the diffuse p functions. Although the large percentage increase in the EBE of the dimer in going from the KT or ΔSCF levels of theory to the EOM-CCSD method would seem to indicate that electron correlation effects are far more important than electrostatic interactions for the binding of the excess electron, it is instructive to consider the results of one-electron model Hamiltonian[38] calculations on the dimer as this approach allows us to evaluate the various contributions to the EBE. These calculations give attractive electrostatic and polarization contributions to the EBE of 267 and 134 meV, respectively, while the repulsive kinetic energy and pseudopotential contributions are −305 and −66 meV, respectively. In interpreting these results, it is important to recognize that the polarization potential in the one-electron model Hamiltonian recovers correlation effects between the excess electron and the electrons of the cluster that are present in a many-electron treatment. Thus, analysis of the various contributions to the EBE in the model Hamiltonian calculation is based on an orbital whose binding energy and charge distribution were determined in the presence of correlation effects. This analysis reveals that when correlation effects are included the electrostatic contribution to the EBE is found to be substantial.

Figure 2 reports for R' values ranging from 9.5 to 70.0 Å the EOM-CCSD EBEs of the A_g and B_{2u} anion states of the $(H_2O)_4$ model. As expected, for large values of R', the two anion states are essentially degenerate, with EBEs being close to that of an individual dimer. The EBE of the A_g anion state decreases slightly as R' is reduced from 40.0 to about 18.5 Å due to a weakening of the electrostatic potential as R' is reduced and then increases as R' is further decreased to 9.5 Å due to a growing correlation contribution. In contrast, the EBE of the B_{2u} anion is found to decrease monotonically as R' decreases, with the anion ceasing to be bound for $R' \lesssim 9.5$ Å. However, we expect that the B_{2u} anion will continue to exist as a TA for R' values less than ∼9.5 Å. On the basis of the analytic structure of the S matrix,[39] one also expects a virtual state at negative energy when the anion is weakly bound. (However, the virtual state cannot be identified from the stabilization/analytic continuation method that we employ.) At the R' value at which the anion just ceases to bind, the poles in the S matrix associated with the bound and virtual states coincide at zero energy. As R' is further decreased, the poles move into the complex energy plane corresponding to the resonance on the physical and unphysical energy sheets.

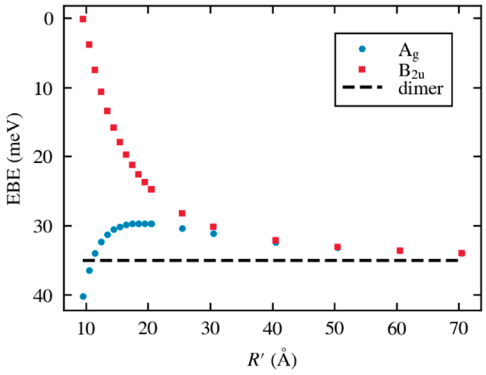

Figure 2. Electron binding energies of the A_g (blue dots) and B_{2u} (red squares) anion states of the $(H_2O)_4$ cluster model as a function of the distance R' separating the two dimers. The EBEs are obtained from EOM-CCSD calculations using the aug-cc-pVTZ basis set augmented with two sets of 9s GTO basis functions located at $\pm (R'/2 + 2.27)$ in Å. The horizontal dashed line indicates the EBE of the dimer subunit.

In order to characterize the charge distributions of the two anion states at a geometry (R' = 13.5 Å) at which both anions are bound, we have calculated the natural orbitals (NOs) associated with "singly occupied" orbitals of the A_g and B_{2u} anion states as described by the EOM-CCSD method. These NOs are shown in Figure 3, from which it is seen that both anion states are highly extended spatially and are decidedly nonvalence-like.

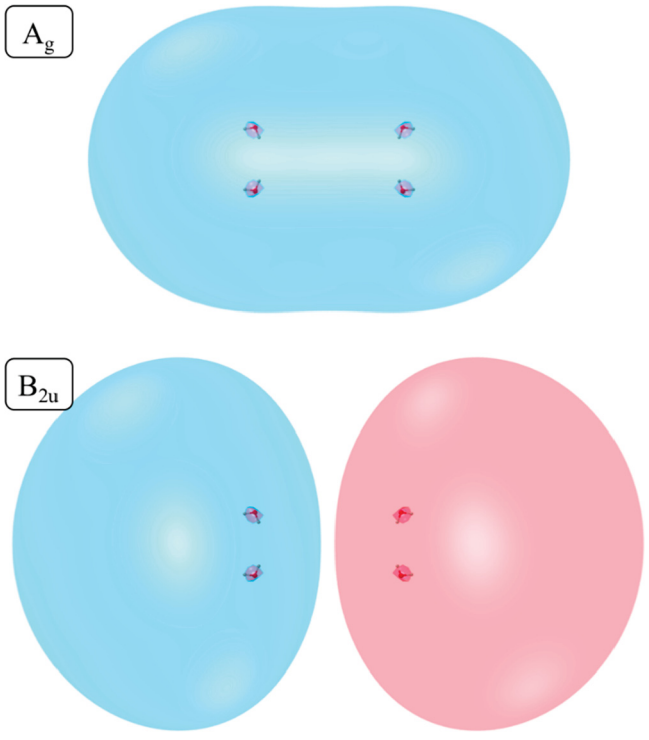

Figure 3. NOs associated with the excess electron of the A_g (upper) and B_{2u} (lower) anions states of the $(H_2O)_4$ cluster model at R' = 13.5 Å and characterized by EOM-CCSD calculations using the aug-cc-pVTZ basis set augmented with two sets of 9s functions as described in the text. The contours shown enclose 90% charge of the charge density.

DOI: 10.1021/acs.jpca.8b11881
J. Phys. Chem. A XXXX, XXX, XXX−XXX

In searching for a B_{2u} TA state for the $(H_2O)_4$ model with $R' \leq 9.0$ Å, we make use of the stabilization method.[40−43] The basic idea of the stabilization method is that a shape resonance can be viewed as a discrete state coupled to the continuum associated with the neutral molecule plus a free electron. In a diabatic picture, in which the coupling between the discrete state and continuum is suppressed, large basis set calculations on the excess electron system give eigenvalues corresponding to the discrete state as well as a series of discretized continuum (DC) levels. If one then scales a parameter that controls the radial extent of the basis set, the energy of the discrete state stays nearly constant, while the energies of the DC levels drop rapidly in energy with increasing extent of the basis set. In an adiabatic picture, the discrete state and the DC states mix, leading to a series of avoided crossings as the scaling parameter is varied.

In the Siegert picture, a resonance is characterized by the complex energy, $E_r - i\Gamma/2$, where E_r is the real part of the resonance energy and Γ, the width, is the reciprocal of the lifetime in atomic units.[44] By use of analytic continuation methods, one can use data from the avoided crossing regions of the stabilization graph (i.e., the plot of the energies vs the scale parameter) to obtain the real energies and the widths of the resonances.[41−43] In our application of the stabilization method to the $(H_2O)_4$ model, we use the EOM-CCSD method together with the aug-cc-pVTZ atomic basis set augmented with two sets of diffuse s functions located as described in section 2. A scale parameter, β, is included in the exponents of the supplemental diffuse basis functions, and to generate the stabilization graphs, β values ranging from 0.2 to 1.7 are used. The two tightest functions in the supplemental 7s set with exponents of 0.025 and 0.0079 make a sizable contribution to the anion wave functions. As a result, the use of scale factors as small as 0.2 necessitated the addition of s GTOs with exponents of 0.0790 and 0.250 to the 7s set described above.

The stabilization graphs for B_{2u} symmetry excess electron states of the $(H_2O)_4$ model at R' = 7.96, 6.46, and 4.46 Å are depicted in Figure 4. The figure also includes the energies of the DC levels calculated using Gaussian 16[45] by setting the nuclear charges equal to zero and solving for the eigenvalues of the single-electron system using the same basis set as used for the EOM-CCSD calculations. Over the energy range considered in stabilization graph for R' = 7.96 Å, the EOM calculations give four eigenvalues while there are only three DC levels. The appearance of an additional eigenvalue in the EOM calculations compared to the number of DC levels indicates the presence of a metastable anion state. It is also seen from this figure that the energy of the lowest eigenvalue from the EOM calculations corresponds closely to that of the lowest DC level. For small values of β, the second DC level also corresponds closely with the second eigenvalue from the EOM calculations. However, for β values larger than about 0.6, the energy of the second eigenvalue from the EOM calculations starts to level off to a value of ∼6 meV, while the energy of the DC level continues to increase linearly. This indicates that for this R' value the resonance occurs near 6 meV. A similar analysis of the stabilization graph for R' = 6.46 Å shows that the resonance in that case occurs between 10 and 15 meV. The stabilization graph for R' = 4.46 Å shows a much broader crossing, with the lowest two eigenvalues from the EOM calculation closely paralleling the DC solutions and the third eigenvalue from the EOM calculation falling slightly

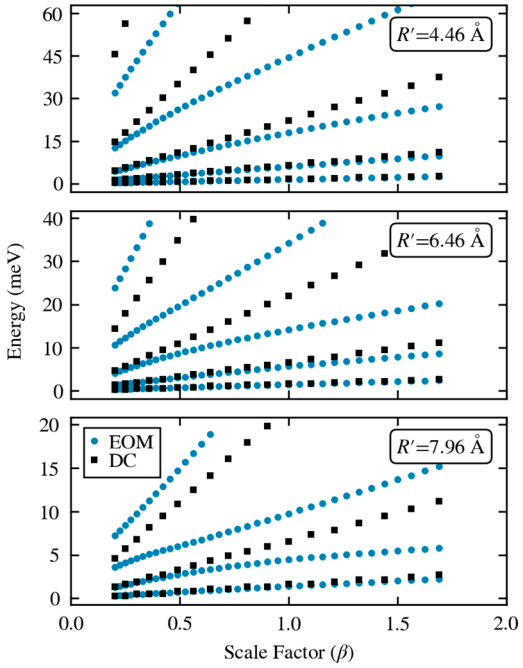

Figure 4. Stabilization graph for $(H_2O)_4$ with R' = 4.46 (top), 6.46 (middle), and 7.96 Å (bottom). The energies of the excess electron states from EOM-CCSD calculations are shown as blue dots, and the energies of the DC levels are shown as black squares.

below the DC solution for larger-scale factors. The fourth eigenvalue from the EOM calculations corresponds to the DC solution only for the smallest scale factors, with a decrease in the slope beginning at around β = 0.5. However, the energy does not plateau, as was the case for R'= 6.46 and 7.96 Å. Thus, for small values of R', it becomes increasingly difficult to ascertain the real part of the resonance energy by simple inspection of the stabilization graph.

In order to extract accurate values for the resonance position (i.e., E_r) and width, we used an analytic continuation method, originally introduced by one of the authors,[46] which, in the limit of a well-isolated avoided crossing between two eigenvalues, fits the energy to

$$PE^2 + QE + R = 0 \quad (1)$$

where P, Q, and R are polynomials in the scale parameter β, i.e.

$$P = 1 + p_1\beta + p_2\beta^2 + \ldots$$
$$Q = q_0 + q_1\beta + q_2\beta^2 + \ldots$$
$$R = r_0 + r_1\beta + r_2\beta^2 + \ldots \quad (2)$$

For systems with narrow resonances, i.e., with $\Gamma/2 \ll E_r$, stabilization graphs generally display well-defined avoided crossings between the diabatic discrete state and the DC solutions as the scale parameter is varied. However, when $\Gamma/2$ is not much less than E_r, the avoided crossings become less pronounced. This is the case for the stabilization graphs for the B_{2u} anion of the $(H_2O)_4$ cluster model, particularly at small R' values, necessitating a generalization of eq 1 to include terms of higher order in E. In this work, terms through E^5 were used in the analytic continuation for R' values less than 7 Å, while terms through E^3 or E^4 were used for larger R' values. The complex energy associated with the resonance is located by solving for the stationary point at which $dE/d\beta = 0$. The

DOI: 10.1021/acs.jpca.8b11881
J. Phys. Chem. A XXXX, XXX, XXX−XXX

resulting complex value of β is substituted into eq 1 or its extension including higher powers of E to determine the real and imaginary parts of the resonance energy. The imaginary part corresponds to $-\Gamma/2$. In our application of this approach to extract resonance parameters of the B_{2u} anion, we employed fits where the polynomials were of order n minus the power of E in the prefactor. To obtain well-converged results, we found it necessary to use $n = 4$ or 5 and to use data from all of the interacting roots over the β range considered. Typically, more data points were used than parameters in combination with least-squares fitting. In addition, for each value of R', several independent analytic continuation calculations using different sets of data points were performed, each giving slightly different complex resonance energies, allowing us to assign error bars to the resulting values of E_r and Γ. In general, the uncertainties in the resonance parameters increase with growing width. For $R' = 7.96$ Å, the stabilization calculations using energies from the EOM-CCSD calculations give resonance parameters of $E_r = 5.36$ ($\pm$0.06) meV and $\Gamma = 2.2$ meV ($\pm$0.1), while at $R' = 6.46$ Å, the resonance parameters are $E_r = 11.0$ ($\pm$0.3) meV and $\Gamma = 8.0$ ($\pm$0.7) meV (the standard deviations from the analytic continuation procedure are given in parentheses as a measure of the uncertainty arising from that procedure but do not reflect errors arising from use of a finite basis set or incomplete recovery of electron correlation).

Valence-type TAs can usually be located by application of the stabilization method at the KT level, i.e., using virtual orbitals from Hartree–Fock calculations on the neutral molecule. This approach, sometimes referred to as the stabilized Koopmans' theory (SKT) approximation,[47] gives resonance positions and widths appreciably larger than the corresponding quantities obtained from methods such as EOM-CCSD that treat electron correlation effects in a balanced manner. Due to the importance of electron correlation effects for the EBE of the B_{2u} anion at R' values for which it is bound, we expected that it would not be possible to locate the corresponding TA in SKT calculations. In fact, at least for R' values for which the EOM-CCSD calculations give a value of Γ considerably smaller than E_r, we find that SKT calculations indicate the presence of a very broad resonance much higher in energy than that found in the EOM-CCSD calculations. For $R' = 7.96$ Å, the SKT calculations give $E_r \approx 230$ meV and $\Gamma \approx 220$ meV, as compared to the corresponding EOM-CCSD values of 5.4 and 2.2 meV. The identification of the resonance at the SKT level has implications for the trapping mechanism, which will be discussed below.

Figure 5 presents the real and imaginary parts of the resonance energy for values of R' ranging from 3.46 to 8.96 Å. In addition, the energy of the B_{2u} state is shown for larger R' values for which the state is bound and has a real-valued energy. The resonance is seen as a continuation of the bound state to positive attachment energies. For most R' values considered, the analytic continuation calculations using different sets of data points gave very similar values of the resonance parameters. However, for some of the R' values at which Γ is comparable to E_r, the analytic continuation calculations using different data points gave significantly different values for the stationary point and, hence, for the resonance parameters. While the averaged values of E_r and Γ from these calculations are in line with those from neighboring R' values, the large spread in the resonance parameters from the different fits of the data leads to large standard deviations.

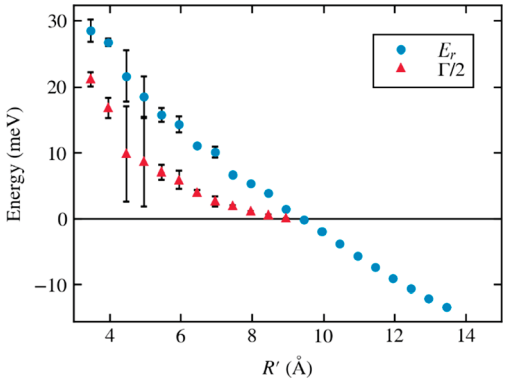

Figure 5. Resonance energy, E_r, (blue dots) and half-width, $\Gamma/2$, (red triangles) from stabilization calculations using EOM-CCSD energies of the B_{2u} anion of the $(H_2O)_4$ model as a function of R'. The figure also includes the negative of the EBE for R' values for which the anion is bound.

For the smallest values of R' considered, the imaginary part is more than half of the real part of the resonance energy, which means that the resonance would extend to threshold.

In order to understand the formation of the B_{2u} state in terms of the various contributions to the electron–molecule interaction potential, it is useful to convert the three-dimensional potential for the interaction of a negative point charge with the cluster to an effective radial potential, depending only on the distance, r, between the electron and the center of mass of the cluster. Neglecting the electrostatic contribution and assuming a spherically symmetric polarization potential, the effective long-range electron–molecule interaction potential is of the form

$$V_{\text{eff}}(r) = -\frac{\alpha}{2r^4} + \frac{l(l+1)}{2r^2} \tag{3}$$

where α is the polarizability and l is the angular momentum quantum number. The r value of the maximum, r_{max}, of the confining potential occurs at

$$r_{\text{max}} = \sqrt{\frac{2\alpha}{l(l+1)}} \tag{4}$$

The existence of a nonvalence resonance in a particular angular momentum channel requires that the confining barrier be peaked at a radial distance that is large compared to the molecule or cluster of interest. In the case of the $(H_2O)_4$ cluster model with $R' = 7.96$ Å and $l = 1$, r_{max} occurs near 3.5 Å, which is far too small to be consistent with a nonvalence shape resonance.

We now consider the impact of including the nonspherical electrostatic contribution to the interaction potential using the protocol of Bordman et al.[48] in which the interaction potential is decomposed into contributions from different spherical harmonics. Assuming that the resonance is purely p-wave in nature, only V_0 and V_2 components can contribute to the effective radial potential. The interaction potential was derived by calculating at the MP2 level the interaction energies of a negative point charge at various in-plane locations relative to the cluster using the same basis set as that used for the stabilization calculations. The electrostatic contribution to the effective potential was calculated separately, and the polarization potential was obtained by subtracting the electrostatic potential from the net potential at each location considered for

DOI: 10.1021/acs.jpca.8b11881
J. Phys. Chem. A XXXX, XXX, XXX–XXX

the point charge. Figure 6 plots the resulting approximate effective radial potential (retaining only the V_0 and V_2 terms in the expansion) for p-wave electron scattering from the $(H_2O)_4$ cluster model with R' = 7.96 Å. From this figure, it is seen that with the inclusion of the electrostatic contribution V_{eff} crosses zero near R' = 15 Å and the maximum in the barrier (≈4.8 meV) in the effective potential occurs near 24 Å. We note also that if the effect of the V_4 term in the expansion on V_0 and V_2 terms is included, the barrier in the effective radial potential is further increased to 7 meV. These results are consistent with the prediction of the EOM-CCSD calculations of a B_{2u} resonance near 5 meV having a highly diffuse charge distribution. We have solved the Schrödinger equation associated with V_{eff} shown in Figure 6 and find that it predicts the anion to be weakly bound rather than metastable, but this is not surprising as V_{eff}, generated as described above, ignores exchange between the excess electron and the electrons of the water molecules as well as orthogonalization effects (but neither of these effects is important for the long-range behavior of the potential). From Figure 6, it is also seen that both electrostatics and polarization effects are important for generating the attractive well, but that polarization is inconsequential in the region of the barrier. The position of the TA as located in the SKT calculations is about 225 meV above the barrier in V_{eff}. A resonance with the E_r and $\Gamma/2$ values predicted by the SKT calculations would be difficult to detect experimentally as the phase shift change would be gradual and would be far less than π as one sweeps through the resonance. Electron correlation effects lower the resonance position by about 225 meV, which places it just below the barrier in the effective potential as estimated above, leading to a significant decrease in the width.

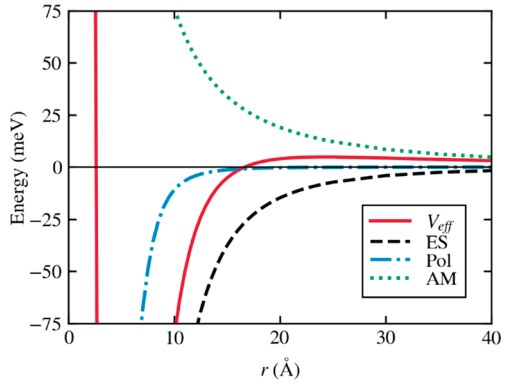

Figure 6. Effective radial potential, V_{eff} (solid red line), vs r, the distance from the center of the cluster, for p-wave scattering from the $(H_2O)_4$ cluster model with R' = 7.96 Å. The electrostatic contribution (ES) is shown as the dashed black line, the polarization contribution (Pol) is shown as the blue dot−dashed line, and the angular momentum contribution (AM) is shown as the green dotted line.

Having examined the effective radial potential for the electron−cluster interaction, it is instructive to consider the charge distribution of the TA. Figure 7 displays the singly occupied NO from EOM-CCSD calculations on the B_{2u} anion state of the $(H_2O)_4$ cluster model at three different R' values. For R' = 9.46 Å, at which the anion is bound, and for R' = 8.96 Å, at which it is metastable, the NO displayed is for the first root of the EOM calculations, while at R' = 7.96 Å, at which it is also metastable, the NO plotted is that associated with the second root of the EOM calculations. For the two R' values at which the anion is metastable, the results shown were obtained at β = 1.7, at which the appropriate root is in the "plateau" region of the stabilization graph (see Figure 4 for R' = 7.96 Å). In a diabatic picture, one can construct a discrete state that is uncoupled from the continuum. The finite lifetime then results from the coupling of this discrete state to the continuum. To a good approximation, the plateau regions of a stabilization graph correspond to the discrete state. Hence, what is actually depicted for R' = 7.96 and 8.96 Å in Figure 7 is the NO associated with the approximate discrete state (in a diabatic picture) rather than the NO actually associated with the TA. The latter is necessarily complex. Recently, methods for obtaining and plotting complex orbitals for resonance states have been developed, though these require the use of a complex Hamiltonian.[49−51] As seen from Figure 7, the anion charge distribution is highly extended both when it is weakly bound and when it is temporary. For R' = 7.96 Å, the NO associated with the discrete state has a nodal surface about 70 Å from the center of the cluster, which enforces orthogonality to the lower-lying DC level. A plot along the R' axis of the charge density associated with the singly occupied NO of the discrete state for R' = 7.96 Å is peaked near r = 8 Å, consistent with the effective potential shown in Figure 6.

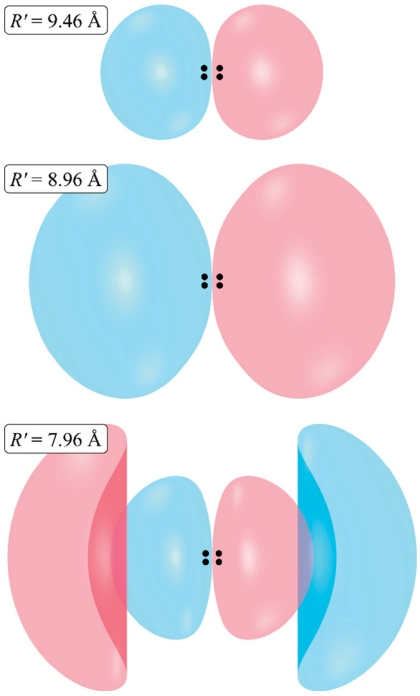

Figure 7. NOs associated with the excess electron of the B_{2u} anion states of the $(H_2O)_4$ cluster model at R' = 9.46, 8.96, and 7.96 Å. The anion is weakly bound at R' = 9.46 Å and is metastable at the two shorter R' values. The NOs are from EOM-CCSD calculations using the aug-cc-pVTZ basis set augmented with two sets of 9s functions, as described in the text. The contours shown enclose 90% of the charge density of the NOs. The black dots indicate the positions of the water molecules.

Although the $(H_2O)_4$ model considered here has a geometry that is unrealizable experimentally, molecules such as $(NaCl)_2$, C_6F_6, tetracyanoethylene, and C_{60} have been predicted to have NVCB anions belonging to the totally symmetric representation at their equilibrium geometries.[5,6,9,17] Thus, these species are candidates for systems with nonvalence shape resonances. Exploratory calculations on $(NaCl)_2$ indeed indicate that this

DOI: 10.1021/acs.jpca.8b11881
J. Phys. Chem. A XXXX, XXX, XXX−XXX

system has a nonvalence TA state of B_{2u} symmetry. For highly polarizable molecules such as C_{60}, there is also the possibility of d-like nonvalence TA states. Nonvalence shape resonances could be detected in an electron scattering experiment. However, this would be challenging given how close such resonances are expected to be to threshold, both because of the finite resolution of electron scattering experiments and because of the impact of the virtual state. A more viable route to their detection would be as resonances in the cross section for photodetachment from the bound ground state anion. At the shortest R' value considered for the $(H_2O)_4$ model, the A_g anion is bound by about 130 meV, and at this R' value, the resonance in the photodetachment cross section would appear near 160 meV or about 1300 cm^{-1}, which would be accessible with a tunable IR laser. For molecules or clusters with a bound valence-type ground state anion, the photodetachment resonances due to nonvalence TAs are likely to fall in the visible or UV. We note also that there is the possibility that a nonvalence TA could be converted into a long-lived nuclear Feshbach resonance[13] in which the excess energy is distributed into vibrational degrees of freedom.

Fossez et al. have considered bound and resonance states of an electron interacting with a linear three-point-charge quadrupole.[52] However, the resonances demonstrated for this point-charge model appear to be fundamentally different from those of the $(H_2O)_4$ cluster model considered here. In particular, the resonances demonstrated in ref 52 have lifetimes orders of magnitude longer than that of the p-wave resonance of the $(H_2O)_4$ cluster model. In addition, electron correlation effects play an important role in establishing the energy and lifetime of the p-wave resonance considered here but are not included in the model Hamiltonian used in ref 52.

4. CONCLUSIONS

In recent years, several studies have appeared demonstrating the existence of nonvalence correlation bound anions of molecules and clusters with no net dipole moment.[5,6,9,17] Nonvalence anion states, whether bound or temporary in nature, have very diffuse charge distributions. For the $(H_2O)_4$ cluster model considered here, both the electrostatic potential (dominated by the quadrupole term) and electron correlation effects are important in establishing the energy position and width of the TA.

We anticipate that nonvalence TAs will exist slightly above threshold for many molecules and clusters that possess NVCB anions. The lowest-energy NVCB anion of a molecule or cluster necessarily belongs to the totally symmetric representation, but the excited nonvalence anion states will necessarily have sizable p or d character, being manifested as TA shape resonances if the electron−molecule potential is not attractive enough to cause these to be bound. Nonvalence TA shape resonances should be detectable as resonances in the photodetachment cross sections from a stable ground state anion, either valence or nonvalence in nature.

AUTHOR INFORMATION

Corresponding Author

*E-mail: Jordan@pitt.edu.

ORCID

Kenneth D. Jordan: 0000-0001-9178-6771

Notes

The authors declare no competing financial interest.

ACKNOWLEDGMENTS

This research was carried out with the support of a grant from the National Science Foundation under Grant CHE1762337. Additional funding was provided by the Grove City College Swezey Fund. The calculations were carried out on computers in the University of Pittsburgh's Center for Research Computing and at Grove City College. We acknowledge helpful discussions with Shiv Upadhyay.

REFERENCES

(1) Desfrançois, C.; Abdoul-Carime, H.; Schermann, J.-P. Ground-State Dipole-Bound Anions. *Int. J. Mod. Phys. B* **1996**, *10*, 1339−1395.
(2) Simons, J.; Jordan, K. D. *Ab Initio* Electronic Structure of Anions. *Chem. Rev.* **1987**, *87*, 535−554.
(3) Wang, F.; Jordan, K. D. Theory of Dipole-Bound Anions. *Annu. Rev. Phys. Chem.* **2003**, *54*, 367−396.
(4) Sommerfeld, T. Multipole-Bound States of Succinonitrile and Other Dicarbonitriles. *J. Chem. Phys.* **2004**, *121*, 4097−4104.
(5) Voora, V. K.; Kairalapova, A.; Sommerfeld, T.; Jordan, K. D. Theoretical Approaches for Treating Non-Valence Correlation-Bound Anions. *J. Chem. Phys.* **2017**, *147*, 214114.
(6) Voora, V. K.; Cederbaum, L. S.; Jordan, K. D. Existence of a Correlation Bound *s*-type Anion State of C_{60}. *J. Phys. Chem. Lett.* **2013**, *4*, 849−853.
(7) Voora, V. K.; Jordan, K. D. Nonvalence Correlation-Bound Anion States of Spherical Fullerenes. *Nano Lett.* **2014**, *14*, 4602−4606.
(8) Voora, V. K.; Jordan, K. D. Nonvalence Correlation-Bound Anion States of Polycyclic Aromatic Hydrocarbons. *J. Phys. Chem. Lett.* **2015**, *6*, 3994−3997.
(9) Voora, V. K.; Jordan, K. D. Non-valence Correlation-Bound Anion State of C_6F_6: Doorway to Low-Energy Electron Capture. *J. Phys. Chem. A* **2014**, *118*, 7201−7205.
(10) Rogers, J. P.; Anstöter, C. S.; Verlet, J. R. R. Ultrafast Dynamics of Low-Energy Electron Attachment via a Non-Valence Correlation-Bound State. *Nat. Chem.* **2018**, *10*, 341−346.
(11) Rogers, J. P.; Anstöter, C. S.; Verlet, J. R. R. Evidence of Electron Capture of an Outgoing Photoelectron Wave by a Nonvalence State in $(C_6F_6)_n^-$. *J. Phys. Chem. Lett.* **2018**, *9*, 2504−2509.
(12) Sommerfeld, T. Coupling between Dipole-bound and Valence States: The Nitromethane Anion. *Phys. Chem. Chem. Phys.* **2002**, *4*, 2511−2516.
(13) Hotop, H.; Ruf, M.-W.; Allan, M.; Fabrikant, I. I. Resonance and Threshold Phenomena in Low-Energy Electron Collisions with Molecules and Clusters. *Adv. At. Mol. Opt. Phys.* **2003**, *49*, 85−216.
(14) Sommerfeld, T.; Dreux, K. M.; Joshi, R. Excess Electrons Bound to Molecular Systems with a Vanishing Dipole but Large Molecular Quadrupole. *J. Phys. Chem. A* **2014**, *118*, 7320−7329.
(15) Sommerfeld, T. Multipole-Bound States of Succinonitrile and other Dicarbonitriles. *J. Chem. Phys.* **2004**, *121*, 4097−4104.
(16) Desfrançois, C.; Bouteiller, Y.; Schermann, J. P.; Radisic, D.; Stokes, S. T.; Bowen, K. H.; Hammer, N. I.; Compton, R. N. Long-Range Electron Binding to Quadrupolar Molecules. *Phys. Rev. Lett.* **2004**, *92*, 083003.
(17) Sommerfeld, T.; Bhattarai, B.; Vysotskiy, V. P.; Cederbaum, L. S. Correlation-Bound Anions of NaCl Clusters. *J. Chem. Phys.* **2010**, *133*, 114301.
(18) Garrett, W. R. Quadrupole-bound Anions: Efficacy of Positive versus Negative Quadrupole Moments. *J. Chem. Phys.* **2012**, *136*, 054116.
(19) Garrett, W. R. Critical Electron Binding to Linear Electric Quadrupolar Systems. *J. Chem. Phys.* **2008**, *128*, 194309.
(20) Compton, R. N.; Dunning, F. B.; Nordlander, P. On the Binding of Electrons to CS_2: Possible Role of Quadrupole-bound States. *Chem. Phys. Lett.* **1996**, *253*, 8−12.

DOI: 10.1021/acs.jpca.8b11881
J. Phys. Chem. A XXXX, XXX, XXX−XXX

(21) Zhu, G.-Z.; Liu, Y.; Wang, L.-S. Observation of Excited Quadrupole-Bound States in Cold Anions. *Phys. Rev. Lett.* **2017**, *119*, 023002.
(22) Abdoul-Carime, H.; Desfrançois, C. Electrons Weakly Bound to Molecules by Dipolar, Quadrupolar or Polarization Forces. *Eur. Phys. J. D* **1998**, *2*, 149−156.
(23) Sommerfeld, T.; Dreux, K. M.; Joshi, R. Excess Electrons Bound to Molecular Systems with Vanishing Dipole but Large Molecular Quadrupole. *J. Phys. Chem. A* **2014**, *118*, 7320−7329.
(24) Koopmans, T. Über die Zuordnung von Wellenfunctionen und Eigenwerten zu den Einzelnen Elektronen Eines Atoms. *Physica* **1934**, *1*, 104−113.
(25) Barsotti, S.; Sommerfeld, T.; Ruf, M. W.; Hotop, H. High Resolution Study of Cluster Anion Formation in Low-energy Electron Collisions with OCS Clusters. *Int. J. Mass Spectrom.* **2004**, *233*, 181−192.
(26) Schulz, G. J. Resonances in Electron Impact on Diatomic Molecules. *Rev. Mod. Phys.* **1973**, *45*, 423−486.
(27) Jordan, K. D.; Burrow, P. D. Studies of the Temporary Anion States of Unsaturated Hydrocarbons by Electron Transmission Spectroscopy. *Acc. Chem. Res.* **1978**, *11*, 341−348.
(28) Jagau, T.-C.; Dao, D. B.; Holtgrewe, N. S.; Krylov, A. I.; Mabbs, R. Same but Different: Dipole-Stabilized Resonances in CuF^- and AgF^-. *J. Phys. Chem. Lett.* **2015**, *6*, 2786−2793.
(29) Skomorowski, W.; Gulania, S.; Krylov, A. I. Bound and Continuum-Embedded States of Cyanopolyyne. *Phys. Chem. Chem. Phys.* **2018**, *20*, 4805−4817.
(30) Carelli, F.; Gianturco, F. A.; Wester, R.; Satta, M. Formation of Cyanopolyyne Anions in the Interstellar Medium: The Possible Role of Permanent Dipoles. *J. Chem. Phys.* **2014**, *141*, 054302.
(31) Møller, C.; Plesset, M. S. Note on an Approximation Treatment for Many-Electron Systems. *Phys. Rev.* **1934**, *46*, 618−622.
(32) Kendall, R. A.; Dunning, T. H., Jr.; Harrison, R. J. Electron Affinities of the First-Row Atoms Revisited. Systematic Basis Sets and Wave Functions. *J. Chem. Phys.* **1992**, *96*, 6796−6806.
(33) Dunning, T. H., Jr. Gaussian Basis Sets for Use in Correlated Molecular Calculations. I. The Atoms Boron through Neon and Hydrogen. *J. Chem. Phys.* **1989**, *90*, 1007−1023.
(34) Stanton, J. F.; Gauss, J. Perturbative Treatment of the Similarity Transformed Hamiltonian in Equation-of-Motion Coupled-Cluster Approximations. *J. Chem. Phys.* **1995**, *103*, 1064−1076.
(35) Stanton, J. F.; Gauss, J.; Harding, M.; Szalay, P. *CFOUR, Coupled-Cluster Techniques for Computational Chemistry*; 2010.
(36) Falcetta, M. F.; Reilly, N. D.; Jordan, K. D. Stabilization Calculations of the Low-Lying Temporary Anion States of Be, Mg, and Ca. *Chem. Phys.* **2017**, *482*, 239−243.
(37) Jagau, T.-C.; Zuev, D.; Bravaya, K. B.; Epifanovsky, E.; Krylov, A. I. A Fresh Look at Resonances and Complex Absorbing Potentials: Density Matrix-Based Approach. *J. Phys. Chem. Lett.* **2014**, *5*, 310−315.
(38) Voora, V. K.; Ding, J.; Sommerfeld, T.; Jordan, K. D. A Self-Consistent Polarization Potential Model for Describing Excess Electrons Interacting with Water Clusters. *J. Phys. Chem. B* **2013**, *117*, 4365−4370.
(39) Domcke, W. Analytic Theory of Resonances, Virtual States and Bound States in Electron-Molecule Scattering and Related Processes. *J. Phys. B: At. Mol. Phys.* **1981**, *14*, 4889−4922.
(40) Hazi, A. U.; Taylor, H. S. Stabilization Method of Calculating Resonance Energies: Model Problem. *Phys. Rev. A* **1970**, *1*, 1109−1120.
(41) McCurdy, C. W.; McNutt, J. F. On the Possibility of Analytically Continuing Stabilization Graphs to Determine Resonance Positions and Widths Accurately. *Chem. Phys. Lett.* **1983**, *94*, 306−310.
(42) Chao, J. S.-Y.; Falcetta, M. F.; Jordan, K. D. Application of the Stabilization Method to $N_2^-(1^2\Pi_g)$ and $Mg^-(1^2P)$ Temporary Anion States. *J. Chem. Phys.* **1990**, *93*, 1125−1135.
(43) Jordan, K. D.; Voora, V. K.; Simons, J. Negative Electron Affinities from Conventional Electronic Structure Methods. *Theor. Chem. Acc.* **2014**, *133* (1445), 1−15.
(44) Siegert, A. J. On the Derivation of the Dispersion Formula for Nuclear Reactions. *Phys. Rev.* **1939**, *56*, 750−752.
(45) Frisch, M. J.; Trucks, G. W.; Schlegel, H. B.; Scuseria, G. E.; Robb, M. A.; Cheeseman, J. R.; Scalmani, G.; Barone, V.; Petersson, G. A.; Nakatsuji, H.; et al. *Gaussian 16*, revision B.01; Gaussian, Inc.: Wallingford, CT, 2016.
(46) Jordan, K. D. Applications of Analytic Continuation in the Construction of Potential Energy Curves. *Int. J. Quantum Chem.* **1975**, *9*, 325−336.
(47) Falcetta, M. F.; Jordan, K. D. Assignments of the Temporary Anion States of the Chloromethanes. *J. Phys. Chem.* **1990**, *94*, 5666−5669.
(48) Boardman, A. D.; Hill, A. D.; Sampanthar, S. Partial Wave Scattering by Non-Spherically Symmetric Potentials. I. General Theory of Elastic Scattering. *Phys. Rev.* **1967**, *160*, 472−475.
(49) White, A. F.; McCurdy, C. W.; Head-Gordon, M. Restricted and Unrestricted Non-Hermitian Hartree-Fock: Theory, Practical Considerations, and Applications to Metastable Molecular Anions. *J. Chem. Phys.* **2015**, *143*, 074103.
(50) Jagau, T.-C.; Krylov, A. I. Characterizing Metastable States Beyond Energies and Lifetimes: Dyson Orbitals and Transition Dipole Moments. *J. Chem. Phys.* **2016**, *144*, 054113.
(51) Skomorowski, W.; Krylov, A. I. Real and Imaginary Excitons: Making Sense of Resonance Wave Functions by Using Reduced State and Transition Density Matrices. *J. Phys. Chem. Lett.* **2018**, *9*, 4101−4108.
(52) Fossez, K.; Mao, X.; Nazarewicz, W.; Michel, N.; Garrett, W. R.; Ploszajczak, M. Resonant Spectra of Quadrupolar Anions. *Phys. Rev. A* **2016**, *94*, 032511.

DOI: 10.1021/acs.jpca.8b11881
J. Phys. Chem. A XXXX, XXX, XXX−XXX